Giant LO-TO Splittings in Perovskite Ferroelectrics

W. Zhong, R.D. King-Smith,* and David Vanderbilt
Department of Physics and Astronomy, Rutgers University, Piscataway, New Jersey 08855-0849
(Received 30 November 1993)

We perform a first-principles investigation of the role of Coulomb interactions in eight ABO_3 cubic perovskite compounds. The predicted spontaneous polarization and the LO and TO phonon frequencies are found to be in good agreement with experiment. Anomalously large dynamical effective charges give rise to very strong mixing of the mode eigenvectors on going from the TO to the LO case, resulting in a "giant LO-TO splitting" in the sense that the soft TO mode is most closely related to the hardest LO modes. The results help explain the extreme sensitivity of these compounds to electrostatic boundary conditions.

PACS numbers: 77.84.Dy, 63.20.Dj, 77.22.Ej

Ferroelectric materials are characterized by a switchable macroscopic polarization. Their importance stems not only from technological considerations, but also from a fundamental interest in understanding the structural phase transitions and symmetry breaking involved [1]. The perovskite compounds are an extremely important group of ferroelectric materials. Their simple structures allow extensive theoretical investigation. The ferroelectric transition occurs as a result of a delicate balance between long-range Coulomb interactions and short-range forces. Of particular interest is the fact that the long range of the Coulomb interaction can make the ferroelectric instability very sensitive to details of domain structure, defects, and boundary conditions. The splitting between the frequencies of the longitudinal optical (LO) and transverse optical (TO) phonons is another direct effect of such interaction. The Born dynamical effective charges, which reflect the local dipole moments which develop as atoms are moved, play a central role in the study of these Coulomb effects.

The role of Coulomb interactions in perovskites aroused interest as early as the 1960s. The seminal work by Axe suggested anomalous effective charges, based on empirical fitting to experimental mode strengths [2]. However, the quantitative accuracy of that approach is limited by the approximations involved, and by uncertainties in the interpretation of experiment. It is natural to turn to first-principles calculations for a deeper understanding and more accurate predictions. However, early band-structure calculations [3] and more recent work focusing on total energies [4–8] do not directly address the role of Coulomb interactions. In part, this is because a method for direct calculation of electric polarization has only recently become available [9]. Recent work using this new method [10] and linear response theory [11] confirmed anomalous effective charges, but the results were limited to two compounds, and their effects on the dynamical properties and soft phonon instability were not addressed.

In this Letter, we report a systematic series of first-principles calculations of Born effective charges Z^* and their effect on the optical phonon modes. We find the anomalously large Z^* to be a general feature of perovskite compounds. This leads to large spontaneous polarization for small distortions. Our calculated optical phonon frequencies at the Γ point for both TO and LO modes are in good agreement with experiment. The eigenvector analysis reveals that, in general, there is no correspondence between individual TO and LO modes. However, the softest TO mode usually involves the largest mode effective charge and can couple strongly with the electric field, thus giving an unexpectedly large LO-TO splitting. The strong coupling to the electric field can easily destroy the ferroelectric state. We find that the calculated critical depolarization factor is only ≈ 0.1. This explains the remarkable sensitivity of the ferroelectric state to domain structure and boundary conditions.

The perfect perovskite structure shown in Fig. 1 is cubic with general formula ABO_3, where A and B are metal atoms. We concentrate on eight perovskite compounds: $BaTiO_3$, $SrTiO_3$, $CaTiO_3$, $KNbO_3$, $NaNbO_3$, $PbTiO_3$, $PbZrO_3$, and $BaZrO_3$. We begin with a calculation of

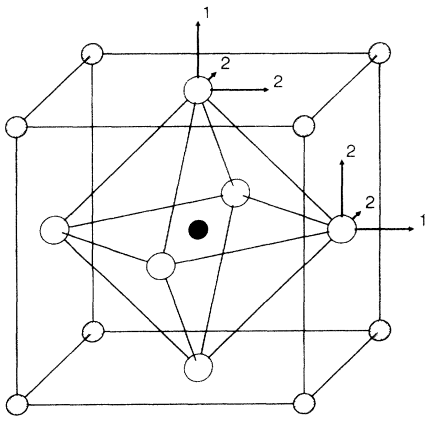

FIG. 1. The structure of cubic perovskite compounds ABO_3. Atoms A, B, and O are represented by shaded, solid, and empty circles, respectively. The small vectors indicate two inequivalent directions for the O atoms.

0031-9007/94/72(22)/3618(4)$06.00

the Born effective charges from finite differences of the bulk polarization $\mathbf{P}$ under small distortions. The Born effective charge tensor $\mathbf{Z}^*_m$ is defined through the equation

$$\delta\mathbf{P} = \frac{e}{\Omega}\sum_{m=1}^{\mathcal{N}} \mathbf{Z}^*_m \cdot \delta\mathbf{u}_m \,. \quad (1)$$

Here, $\mathcal{N}$ is the number of atoms in the primitive unit cell, $\delta\mathbf{u}_m$ is the first-order change of the position vector of the mth basis atom, and Ω is the volume of the unit cell. Resta *et al.* [10] have shown that $\mathbf{P}$ is linear in $\mathbf{u}_m$ to a good approximation.

The calculation of polarization follows the new procedure recently introduced in Ref. [9]. The electronic wave functions are obtained from density-functional theory in the local density approximation (LDA), using Vanderbilt's ultrasoft pseudopotential [9,12,13], which allows highly accurate calculations to be performed with a low energy cutoff. A generalized Kohn-Sham functional [8,14] is directly minimized using a preconditioned conjugate gradient method [8,15]. Calculations of structural properties and convergence tests have been presented previously [8]. The electronic polarization $\mathbf{P}$ is calculated using a $4 \times 4 \times 20$ k-point mesh with the dense grid in the direction parallel to $\mathbf{P}$ to achieve high accuracy. The effective charge tensors for the ABO_3 perovskite compounds are then calculated from the polarization differences between perfect and distorted structures.

For the cubic structure, the metal atoms A or B are located at centers of cubic symmetry, so that their effective charge tensors are isotropic. The oxygen atoms are located at the face centers and thus have two inequivalent directions either perpendicular or parallel to the cubic face, labeled 1 or 2, respectively, in Fig. 1. The oxygen effective charge tensors are thus diagonal, with element Z^*_1 for direction 1 and Z^*_2 for directions 2. Since the formulation we use here satisfies the acoustic sum rule $\sum_m \mathbf{Z}^*_m = 0$ exactly, we need three distorted structures to get all the $\mathbf{Z}^*_m$'s. The amplitudes of our distortions are typically 0.2% of the lattice constants.

The calculated Born effective charges are listed in Table I, together with results from other groups. Our results are in good agreement with previous calculations for $KNbO_3$ using finite differences of polarization [10], and for $BaTiO_3$ using variational linear-response theory [11]. The agreement with the empirical approach of Axe [2] is also surprisingly good, suggesting that his modeling was reasonable. The calculations were performed in the theoretical cubic structures. In two cases, we also did the calculations for experimental tetragonal structures, showing that the $\mathbf{Z}^*$ are quite insensitive to structural details.

As shown in Table I, the anomalously large $Z^*(B)$ and $Z^*_1(\mathrm{O})$ reported previously for $KNbO_3$ [10] and $BaTiO_3$ [11] are generic to all the perovskites studied here. However, with the exception of the Pb compounds, $Z^*(A)$ and $Z^*_2(\mathrm{O})$ are close to their nominal ionic valence (+1 for Na and K, +2 for Ca, Sr, and Ba, and −2 for O). We find a strong correlation between the effective charge and chemical species of the metal atoms, i.e., $Z^*(B)$ is independent of A and vice versa. For example, Z^*(Ti) are 7.16, 7.12, 7.08, and 7.06, in compounds $BaTiO_3$, $SrTiO_3$, $CaTiO_3$, and $PbTiO_3$, respectively. Another observation is the strong correlation between $Z^*(B)$ and $Z^*_1(\mathrm{O})$, as well as between $Z^*(A)$ and $Z^*_2(\mathrm{O})$. This is obviously associated with the fact that displacement O_1 modulates the O-B bond, while O_2 modulates the O-A bond.

TABLE I. Born effective charges for ABO_3 perovskites. $Z^*_1(\mathrm{O})$ and $Z^*_2(\mathrm{O})$ refer to O displacements 1 and 2 of Fig. 1.

	$Z^*(A)$	$Z^*(B)$	$Z^*_1(\mathrm{O})$	$Z^*_2(\mathrm{O})$	Structure
$BaTiO_3$	2.75	7.16	−5.69	−2.11	Cubic
	2.70	7.10	−5.56	−2.12	Cubic[a]
	2.9	6.7	−4.8	−2.4	Cubic[b]
$SrTiO_3$	2.54	7.12	−5.66	−2.00	Cubic
	2.4	7.0	−5.8	−1.8	Cubic[b]
$CaTiO_3$	2.58	7.08	−5.65	−2.00	Cubic
$KNbO_3$	1.14	9.23	−7.01	−1.68	Cubic
	1.14	9.36	−7.10	−1.70	Tetragonal
	0.82	9.13	−6.58	−1.68	Tetragonal[c]
$NaNbO_3$	1.13	9.11	−7.01	−1.61	Cubic
$PbTiO_3$	3.90	7.06	−5.83	−2.56	Cubic
	3.92	6.71	−5.51	−2.56	Tetragonal
$PbZrO_3$	3.92	5.85	−4.81	−2.48	Cubic
$BaZrO_3$	2.73	6.03	−4.74	−2.01	Cubic

[a]Reference [11], using density functional perturbation theory.
[b]Reference [2], empirical approach.
[c]Reference [10], using finite differences of polarization.

The anomalously large values of $Z^*(B)$ and $Z^*_1(\mathrm{O})$ indicate that a strong dynamic charge transfer takes place along the O-B bond as the bond length is varied. This can be understood as arising from the weakly ionic character of the bond as follows. At rest, the bonding orbital has most of its character on the O $2p$ orbital; but as it is compressed and the hopping integral increases, the bond becomes more covalent, and the admixture of B d character increases, corresponding to an electron transfer from O to B [16]. It is easily seen that this effect will be strongest for bonds which are on the borderline between ionic and covalent behavior. Thus, we suspect that such anomalous Z^* values will be generic to weakly ionic oxides.

The effective charges can be used to predict the spontaneous polarization P_s for ferroelectric or antiferroelectric materials, given the ground state structure. As a test, we calculate P_s for some structures and compare with experiment. All the structural information is obtained from *Landolt-Bornstein* [17]. For $BaTiO_3$, the calculated P_s are 0.30, 0.26, and 0.44 C/m^2 for tetragonal, orthorhombic, and rhombohedral phases, compared with experimental values of 0.27, 0.30, and 0.33 C/m^2, respectively [18]. The agreement is very good, except for the rhombohedral phase, where the complicated twinning effect in the sample may have caused the too small observed P_s [18]. For $KNbO_3$ in the tetragonal phase, the

calculated $P_s = 0.40$ C/m^2 is in good agreement with the experimental result of 0.40 C/m^2. We calculated P_s for $PbTiO_3$ in the tetragonal structures for two different temperatures; the resulting values are 1.04 C/m^2 at 295 K, and 0.74 C/m^2 at 700 K, to be compared with experimental values of 0.75 and 0.50 C/m^2, respectively [19]. We suspect these discrepancies may be related in part to cracking and charge leakage problems in the experiment [17].

The Born effective charge tensor reflects the effect of Coulomb interactions and is directly related to the LO-TO splitting. The dynamical matrix can be shown to take the form [20]

$$D_{\mu\nu}^{mn}(\mathbf{q}) = D_{\mu\nu}^{(0)mn}(\mathbf{q}) + \frac{4\pi e^2}{\Omega} \frac{(\mathbf{Z}_m^* \cdot \hat{\mathbf{q}})_\mu (\mathbf{Z}_n^* \cdot \hat{\mathbf{q}})_\nu}{\epsilon_\infty(\mathbf{q})} , \quad (2)$$

where $\mathbf{q}$ is the wave vector, $\epsilon_\infty(\mathbf{q})$ is the optical macroscopic dielectric function, and $D^{(0)}$ is an analytic function of $\mathbf{q}$. The difference between the LO and TO frequencies for an ionic crystal arises from the last term in Eq. (2), which accounts for the effect of the macroscopic electric field which is only present for the LO modes.

We are specifically interested in the LO-TO splitting at $\mathbf{q} = 0$. The dynamical matrix $D^{(0)}(\mathbf{q} = 0)$ has been previously calculated in investigating the soft phonon modes [8]. We take experimental values for $\epsilon_\infty(0)$. The observed values in the visible light range [17] are extrapolated to the optical $\omega = 0$ limit using the dispersion relation $\epsilon - 1 = C/(\omega_0^2 - \omega^2)$, where C and ω_0 are constants. The resulting values of $\epsilon_\infty(0)$ are 5.24 ($BaTiO_3$), 5.18 ($SrTiO_3$), 5.81 ($CaTiO_3$), 4.69 ($KNbO_3$), 4.96 ($NaNbO_3$), and 8.64 ($PbTiO_3$). The fact that these experimental values are obtained for the cubic phase at high temperature, or for a lower-symmetry phase, introduces some uncertainty into the calculated LO mode frequencies. We could not find corresponding data for $PbZrO_3$ and $BaZrO_3$.

For the perfect cubic perovskite structure at $\mathbf{q} = 0$, there are 15 phonon modes: 3 acoustic modes, 4 LO modes, and 4 doubly degenerate TO modes. One pair of TO and LO modes are not split by the Coulomb interaction; not being infrared (IR) active, we do not consider them further. The calculated IR-active TO and LO mode frequencies are shown in Table II, together with experimental observed values. The experimental values quoted are either for the F_{1u} modes in the cubic structure, or the corresponding E modes in the tetragonal structure. The agreement with experimental values is typically within 5%–10%, which is very good for an *ab initio* calculation. The less satisfying agreement for $PbTiO_3$ and $PbZrO_3$ is partly due to the big difference between the experimental tetragonal phase and the theoretical cubic phase.

The eigenvector analysis shows that generally there is no correspondence between individual TO and LO phonon modes. For convenience we consider only modes of a given Cartesian polarization, say along $\hat{\mathbf{z}}$, for the remainder of this paper. The dynamical matrices for LO and TO modes at $\mathbf{q} = 0$ are then related by

$$D_{mn}^{\mathrm{LO}} = D_{mn}^{\mathrm{TO}} + \frac{4\pi e^2}{\Omega} \frac{Z_m^* Z_n^*}{\epsilon_\infty(0)} . \quad (3)$$

The correlation between the LO and TO modes can be measured by the matrix $c_{ij} = \langle \xi_i^{\mathrm{TO}} | M | \xi_j^{\mathrm{LO}} \rangle$, where $M_{mn} = M_m \delta_{mn}$ is the mass matrix and ξ_i are the IR-active mode eigenvectors. The c_{ij} matrix for $KNbO_3$ is typical:

$$c = \begin{pmatrix} 0.19 & 0.63 & 0.75 \\ 0.98 & 0.14 & 0.13 \\ 0.03 & 0.76 & 0.65 \end{pmatrix} , \quad (4)$$

where rows label TO modes and columns label LO modes. Note that c_{13} is the largest element in the first row, which means that the *softest TO mode (TO1) is most closely associated with the hardest LO mode (LO3).*

TABLE II. Calculated IR-active optical phonon frequencies (cm^{-1}) in comparison with experimental values. Measured E modes of tetragonal structures are listed for $BaTiO_3$, $PbTiO_3$, and $PbZrO_3$. Imaginary frequencies indicate soft modes.

	TO1		TO2		TO3		LO1		LO2		LO3	
	Theor.	Expt.	Theor.	Expt.	Theor.	Expt.	Theor.	Expt.	Theor.	Expt.	Theor.	Expt.
$BaTiO_3$	178i		177	181[a]	468	487[a]	173	180[a]	453	468[a]	738	717[a]
$SrTiO_3$	41i		165	175[b]	546	545[b]	158	171[b]	454	474[b]	829	795[b]
$CaTiO_3$	153i		188		610		133		427		866	
$KNbO_3$	143i		188	198[c]	506	521[c]	183	190[c]	407	418[c]	899	826[c]
$NaNbO_3$	152i		115		556	535[d]	101		379	411[d]	928	876[d]
$PbTiO_3$	144i		121	210[e]	497	500[e]	104		410		673	750[e]
$PbZrO_3$	131i		63	221[f]	568	508[f]						
$BaZrO_3$	95	115[f]	193	210[f]	514	505[f]						

[a]T. Nakamura, Ferroelectrics **137**, 65 (1992).
[b]J.L. Servoin, Y. Luspin, and F. Gervais, Phys. Rev. B **22**, 5501 (1980).
[c]M.D. Fontana, G. Métrat, J.L. Servoin, and F. Gervais, J. Phys. C **17**, 483 (1984).
[d]F. Gervais, J.L. Servoin, J.F. Baumard, and F. Denoyer, Solid State Commun. **41**, 345 (1982).
[e]Reference [17].
[f]C.H. Perry, D.J. McCarthy, and G. Ruprecht, Phys. Rev. **138**, A1537 (1965).

TABLE III. The effective charges associated with IR-active TO modes. Last column: critical depolarization factor.

	$\bar{Z}$(TO1)	$\bar{Z}$(TO2)	$\bar{Z}$(TO3)	L_c
$BaTiO_3$	8.95	1.69	1.37	0.062
$SrTiO_3$	7.37	3.22	3.43	0.003
$CaTiO_3$	6.25	4.94	4.50	0.112
$KNbO_3$	8.58	1.70	4.15	0.040
$NaNbO_3$	6.95	2.32	5.21	0.071
$PbTiO_3$	7.58	4.23	3.21	0.083
$PbZrO_3$	4.83	4.86	4.30	
$BaZrO_3$	4.01	5.57	3.84	

This remarkable behavior is also clearly evident in the values of the mode effective charges, defined as $\bar{Z}_j^* = \sum_m M_m^{1/2} Z_m^* \xi_{jm}^{\mathrm{TO}}$. If the last term of Eq. (3) did not cause any mixing of the mode eigenvectors, this value would directly reflect the LO-TO splitting. Table III lists the calculated mode effective charges for all 8 compounds. We find that $\bar{Z}^*$ for the soft mode is usually the largest, which means that the soft mode will couple most strongly with the **E** field. In fact, we find that if we construct an LO mode with an eigenvector identical to that of the soft TO mode (TO1), its frequency would generally lie between those of the LO2 and LO3 modes. The extreme case is $BaTiO_3$, for which the LO frequency associated with TO1 is 708 cm^{-1}, only 3% smaller than that of LO3. This giant LO-TO splitting reflects the importance of the Coulomb interaction. Most compounds have a large $\bar{Z}^*$ for more than one mode. These modes will be strongly mixed by the Coulomb interaction in going to the LO case. Since the LO and TO modes have quite different eigenvectors, any model that assumes a one-to-one correspondence between LO and TO modes would be highly unjustified for perovskite compounds.

The role of Coulomb interaction depends on the **E** field inside the material. With no external field, $\mathbf{E} = -4\pi L\mathbf{P}$, where L is the depolarization factor which depends on the geometry of the material ($L = 1/3$ for a sphere, $L = 0$ for a needle, and $L = 1$ perpendicular to a thin film). We calculate the critical depolarization factor L_c, above which the ferroelectric state becomes unstable. It is the value which makes the matrix

$$D_{mn}^{\mathrm{TO}}(0) + L_c \frac{4\pi e^2}{\Omega} \frac{Z_m^* Z_n^*}{\epsilon_\infty(0)} \qquad (5)$$

have a second zero eigenvalue, besides that for translation. The calculated L_c's, listed in Table III, are found to be remarkably small. Thus, it is clear that electric-field effects will be critical and that the boundary conditions and/or domain structures will play a very important role in the occurrence of ferroelectricity. In other words, the ferroelectric state can only develop when the depolarization field is close to zero.

In conclusion, we calculate the effective charge tensors Z^* for cubic perovskite materials ABO_3 using ultrasoft pseudopotentials and a preconditioned conjugate-gradient method. We find, for all the compounds studied, that $Z^*(B)$ and $Z^*(O)$ are anomalously large. The LO and TO phonon frequencies are calculated and found to be in good agreement with experimental observations. The giant LO-TO splittings which emerge from the calculation indicate the importance of Coulomb interactions, resulting in a remarkably small critical depolarization field and a great sensitivity of the ferroelectricity to the domain structure and boundary conditions.

We thank R. Godby and K. Rabe for useful discussions. This work was supported by the Office of Naval Research under Contract No. N00014-91-J-1184.

* Permanent address: Biosym Technologies Inc., 9685 Scranton Rd., San Diego, CA 92122.

[1] M.E. Lines and A.M. Glass, *Principles and Applications of Ferroelectrics and Related Materials* (Clarendon Press, Oxford, 1977).
[2] J.D. Axe, Phys. Rev. **157**, 429 (1967).
[3] L.F. Mattheiss, Phys. Rev. B **6**, 4718 (1972).
[4] R.E. Cohen, Nature (London) **358**, 136 (1992).
[5] K.H. Weyrich and R. Siems, Jpn. J. Appl. Phys. **24**, Suppl. 24-2, 206 (1985).
[6] D.J. Singh and L.L. Boyer, Ferroelectrics **136**, 95 (1992).
[7] R.D. King-Smith and D. Vanderbilt, Ferroelectrics **136**, 85 (1992).
[8] R.D. King-Smith and D. Vanderbilt, Phys. Rev. B **49**, 5828 (1994).
[9] R.D. King-Smith and D. Vanderbilt, Phys. Rev. B **47**, 1651 (1993).
[10] R. Resta, M. Posternak, and A. Baldereschi, Phys. Rev. Lett. **70**, 1010 (1993).
[11] Ph. Ghosez, X. Gonze, and J. -P. Michenaud, in Proceedings of the 8th International Meeting on Ferroelectrics (to be published).
[12] D. Vanderbilt, Phys. Rev. B **41**, 7892 (1990).
[13] K. Laasonen, A. Pasquarello, R. Car, C. Lee, and D. Vanderbilt, Phys. Rev. B **47**, 10 142 (1993).
[14] T.A. Arias, M.C. Payne, and J.D. Joannopoulos, Phys. Rev. Lett. **69**, 1077 (1992).
[15] M.C. Payne, M.P. Teter, D.C. Allan, T.A. Arias, and J.D. Joannopoulos, Rev. Mod. Phys. **64**, 1045 (1992).
[16] W.A. Harrison, *Electronic Structure and the Properties of Solids* (Dover, New York, 1980).
[17] T. Mitsui *et al.*, *Oxides*, Landolt-Bornstein Numerical Data and Functional Relationships in Science and Technology, Group III, Vol. 16, Pt. a (Springer-Verlag, Berlin, 1981); E. Nakamura *et al.*, *ibid.* Group III, Vol. 28 (to be published).
[18] H.H. Wieder, Phys. Rev. **99**, 1161 (1955).
[19] V.G. Gavrilyachenko *et al.*, Fiz. Tverd. Tela **12**, 1532 (1970) [Sov. Phys. Solid State **12**, 1203 (1970)].
[20] R.M. Pick, M.H. Cohen, and R.M. Martin, Phys. Rev. B **1**, 910 (1970).

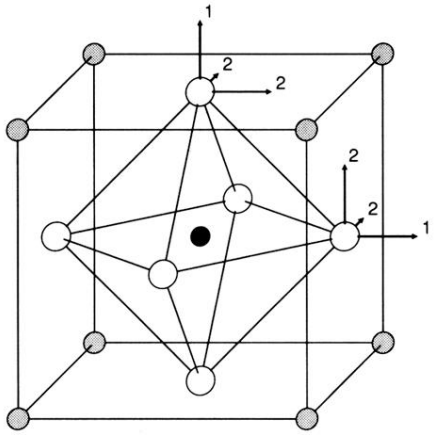

FIG. 1. The structure of cubic perovskite compounds ABO_3. Atoms A, B, and O are represented by shaded, solid, and empty circles, respectively. The small vectors indicate two inequivalent directions for the O atoms.